

# Estimation of States and Parameters of a Drift-Flux Model with Unscented Kalman Filter

Amirhossein Nikoofard\* Ulf Jakob F. Aarsnes\*  
Tor Arne Johansen\*\* Glenn-Ole Kaasa\*\*\*

\* Department of Engineering Cybernetics, Norwegian University of Science and Technology, 7491 Trondheim, Norway  
(Amirhossein.nikoofard@ntnu.no, Ulf.jakob.aarsnes@itk.ntnu.no)

\*\* Center for Autonomous Marine Operations and Systems, Department of Engineering Cybernetics, Norwegian University of Science and Technology, 7491 Trondheim, Norway  
(Tor.arne.johansen@itk.ntnu.no.)

\*\*\* Kelda Drilling Controls (gok@kelda.no).

---

**Abstract:** We present a simplified drift-flux model (DFM) describing a multiphase (gas-liquid) flow during drilling. The DFM uses a specific slip law, without flow-regime predictions, which allows for transition between single and two phase flows. With this model, we design an Unscented Kalman Filter (UKF) for estimation of unmeasured states, production parameters and slip parameters using real time measurements of the bottom-hole pressure and liquid and gas rate at the outlet. The performance is tested against the Extended Kalman Filter (EKF) by using OLGA simulations of typical drilling scenarios. The results show that both UKF and EKF are capable of identifying the production constants of gas from the reservoir into the well, while the UKF has better convergence rate compared with EKF.

*Keywords:* Under-balanced drilling, UKF, Adaptive observer, simplified drift-flux model.

---

## 1. INTRODUCTION

$$q_{influx} = PI \cdot \max(p_{res} - p_{bh}, 0). \quad (3)$$

There have been an increasing research focus on automation of drilling for exploration and production of hydrocarbons in the recent years. Modeling for estimation, and model-based control techniques have been studied in a wide range of drilling and production scenarios. In Managed Pressure Drilling (MPD), a back-pressure pump in conjunction with a back pressure choke is used to control the pressure in the well, posing new control and estimation challenges. In a typical scenario, the control goal is to keep the pressure of the well ( $p_{well}(t, x)$ ) greater than pressure of the reservoir ( $p_{res}(t, x)$ ) to prevent influx from entering the well, but lower than the fracture pressure ( $p_{frac}(t, x)$ ) to avoid the loss of drilling fluids to the reservoir

$$p_{res}(t, x) < p_{well}(t, x) < p_{frac}(t, x) \quad (1)$$

at all times  $t$  and along the well profile  $x \in [0, L]$ .

In an alternative approach, known as Under-Balanced Drilling (UBD), the pressure in the well is kept greater than the collapse pressure of the well but lower than the pressure of the reservoir

$$p_{coll}(t, x) < p_{well}(t, x) < p_{res}(t, x) \quad (2)$$

Due to the pressure drawdown (meaning the positive difference of the reservoir pressure and well pressure) inflow fluid, in many cases gas, is produced continuously from the reservoir. The rate of reservoir inflow is typically approximated mathematically by a so-called Production Index (PI) parameter

Especially for under-balanced wells producing gas, the magnitude of the PI has a significant impact on the dynamics of the UBD and thus also on the control problem. Hence, accurate estimates of the PI and reservoir pressure are important for an UBD operation.

Modeling of UBD operations and MPD scenarios handling influx requires a multiphase model. A popular model in the literature is the Drift-Flux Model (DFM) Evje and Fjelde (2002); Lorentzen et al. (2003); Lage et al. (1999). The drift flux model is a set of first order nonlinear hyperbolic partial differential equations (PDE). In case of two-phase flow, it consists of three governing equations. The Low-Order Lumped (LOL) models are simpler methods that can be used. However, these models are only able to capture the major effects in the well and for the general purpose it produces less accurate results. Nygaard and Nævdal (2006); Nikoofard et al. (2014a); Storkaas et al. (2003).

Due to the complexity of the multi-phase flow dynamics of a UBD well coupled with a reservoir, the modeling, estimation and model based control of UBD operations is still considered an emerging and challenging topic within drilling automation. Nygaard et al. (2006) compared and evaluated the performance of the extended Kalman filter, the ensemble Kalman filter and the unscented Kalman filter based on a low order model to estimate the states and the PI in UBD operation. In Nygaard et al. (2007), a finite horizon nonlinear model predictive control in com-

combination with an unscented Kalman filter was designed for controlling the bottom-hole pressure based on a low order model developed in Nygaard and Nævdal (2006). The unscented Kalman filter was used to estimate the states, and the friction and choke coefficients. Nikoofard et al. (2014a) designed a Lyapunov-based adaptive observer, a recursive least squares estimation and a joint unscented Kalman filter based on a low-order lumped model to estimate states and parameters during UBD operations. A Nonlinear Moving Horizon Observer based on a low-order lumped model was designed for estimating the total mass of gas and liquid in the annulus and geological properties of the reservoir during UBD operation in Nikoofard et al. (2014b).

Lorentzen et al. (2003) designed an ensemble Kalman filter based on the drift-flux model to tune the uncertain parameters of a two-phase flow model in the UBD operation. Vefring et al. (2003, 2006) compared and evaluated the performance of the ensemble Kalman filter and an off-line nonlinear least squares technique utilizing the Levenberg-Marquardt optimization algorithm to estimate reservoir pore pressure and reservoir permeability during UBD while performing an excitation of the bottom-hole pressure. Both methods are capable of identifying the reservoir pore pressure and reservoir permeability. Aarsnes et al. (2014a) used a simplified drift-flux model and an Extended Kalman Filter to estimate the states and PI online, and suggested a scheme combining this with off-line calibration using the algorithm in Vefring et al. (2003). The provided analysis also suggests how such a scheme fits into the UBD operating envelope as proposed by Graham and Culen (2004), and explored in Aarsnes et al. (2014b). Di Meglio et al. (2014) designed an adaptive observer on the DFM.

The problem of parameter estimation in multiphase flows is often referred to as 'soft-sensing' in the context of production, see Luo et al. (2014); Lorentzen et al. (2014); Bloemen et al. (2006); Teixeira et al. (2014); Gryzlov (2011).

The unscented Kalman filter (UKF) has been shown to typically have a better performance than other Kalman filter techniques for nonlinear system (Simon (2006); Wan and van der Merwe (2002)). This paper is the first case of UKF being used with the drift-flux model. This paper presents the design of a UKF based on a simplified drift-flux model to estimate the states, geological properties of the reservoir and slip parameters during UBD operation. The performance of UKF is evaluated against EKF by using measurements from OLGA simulator and the consequences of not estimating slip parameters are discussed. This paper is organized as follows: Section 2 presents the simplified drift-flux model based on mass and momentum balances for UBD operation. Section 3 and 4 explain UKF and EKF for simultaneously estimating the states and parameters of a simplified drift-flux model from OLGA simulator measurements. In the section 5, the simulation results are provided for state and parameter estimation. At the end the conclusion of the paper are presented.

## 2. THE DRIFT FLUX MODEL

The model employed is the same as the one used in Aarsnes et al. (2014b). It expresses the mass conservation law for the gas and the liquid separately, and a combined

momentum equation. The mud, oil and water are lumped into one single liquid phase. In developing the model, the following mass variables are used

$$m = \alpha_L \rho_L, \quad n = \alpha_G \rho_G$$

where for  $k = L, G$  denoting liquid or gas,  $\rho_k$  is the phase density, and  $\alpha_k$  is the volume fraction satisfying

$$\alpha_L + \alpha_G = 1. \quad (4)$$

Further  $v_k$  denotes the velocities, and  $P$  the pressure. All of these variables are functions of time and space. We denote  $t \geq 0$  the time variable, and  $x \in [0, L]$  the space variable, corresponding to a curvilinear abscissa with  $x = 0$  corresponding to the bottom hole and  $x = L$  to the outlet choke position (see Fig. 1). The isothermal equations are as follows,

$$\frac{\partial m}{\partial t} + \frac{\partial m v_L}{\partial x} = 0, \quad (5)$$

$$\frac{\partial n}{\partial t} + \frac{\partial n v_G}{\partial x} = 0, \quad (6)$$

$$\frac{\partial(m v_L + n v_G)}{\partial t} + \frac{\partial(P + m v_L^2 + n v_G^2)}{\partial x} = -(m + n)g \sin \Delta \theta - \frac{2f(m + n)v_m |v_m|}{D}. \quad (7)$$

In the momentum equation (7), the term  $(m + n)g \sin \Delta \theta$  represents the gravitational source term, while

$-\frac{2f(m+n)v_m |v_m|}{D}$  accounts for frictional losses. The mixtures velocity is given as

$$v_m = \alpha_G v_G + \alpha_L v_L. \quad (8)$$

Along with these distributed equations, algebraic relations are needed to describe the system.

### 2.1 Closure Relations

Both the liquid and gas phase are assumed compressible. This is required for the model to handle the transition from two-phase to single-phase flow. The densities are thus given as functions of the pressure as follows

$$\rho_G = \frac{P}{c_G^2}, \quad \rho_L = \rho_{L,0} + \frac{P}{c_L^2}, \quad (9)$$

where  $c_k$  is the velocity of sound and  $\rho_{L,0}$  is the reference density of the liquid phase given at vacuum. Notice that the velocity of sound in the gas phase  $c_G$  depends on the temperature as suggested by the ideal gas law. The temperature profile is assumed to be known.

Combining (9) with (4) we obtain the following relations for finding volume fractions from the mass variables:

$$\alpha_G = \frac{1}{2} - \frac{\frac{c_G^2}{c_L^2} n + m + \sqrt{\Delta}}{2\rho_{L,0}}, \quad (10)$$

$$\Delta = \left(\rho_{L,0} - \frac{c_G^2}{c_L^2} n - m\right)^2 + 4\frac{c_G^2}{c_L^2} n \rho_{L,0} \quad (11)$$

Then the pressure can be found using a modified expression to ensure pressure is define when the gas vanishes

$$P = \begin{cases} \left(\frac{m}{1 - \alpha_G} - \rho_{L,0}\right) c_L^2, & \text{if } \alpha_G \leq \alpha_G^* \\ \frac{n}{\alpha_G} c_G^2, & \text{otherwise.} \end{cases} \quad (12)$$

$\alpha_G^*$  is typically chosen as 0.5. Because the momentum equation (7) was written for the gas-liquid mixture, a so-called *slip law* is needed to empirically relate the velocities

of gas and liquid. To handle the transition between single and two-phase flow, a relation with state-dependent parameters is needed (Evje (2011); Shi et al. (2005)).

$$v_G = (K - (K - 1)\alpha_G)v_m + \alpha_L S \quad (13)$$

where  $K \geq 1$  and  $S \geq 0$  are constant parameters.

### 2.2 Boundary Conditions

Boundary conditions are given by the mass-rates of gas and liquid injected from the drilling rig and flowing in from the reservoir. Denoting the cross sectional flow area by  $A$ , the boundary fluxes are given as:

$$mv_L|_{x=0} = \frac{1}{A} (W_{L,res}(t) + W_{L,inj}(t)), \quad (14)$$

$$nv_G|_{x=0} = \frac{1}{A} (W_{G,res}(t) + W_{G,inj}(t)). \quad (15)$$

The injection mass-rates of gas and liquid,  $W_{G,inj}$ ,  $W_{L,inj}$ , are specified by the driller and can, within some constraints, be considered as manipulated variables. The inflow from the reservoir is dependent on the pressure on the left boundary, for which, within the operational range of a typical UBD operation, an affine approximation should suffice, i.e.

$$W_{L,res} = k_L \max(P_{res} - P(0), 0) \quad (16)$$

$$W_{G,res} = k_G \max(P_{res} - P(0), 0) \quad (17)$$

Here  $P_{res}$  is the reservoir pore pressure and  $k_G, k_L$  are the production index (PI) of the gas and liquid respectively.

The topside boundary condition is given by a choke equation relating topside pressure to mass flow rates

$$\frac{mv_L}{\sqrt{\rho_L}} + \frac{nv_G}{Y\sqrt{\rho_G}} \Big|_{x=L} = \frac{C_v(Z)}{A} \sqrt{\max(P(L,t) - P_s, 0)}, \quad (18)$$

where  $C_v$  is the choke opening given by the manipulated variable  $Z$ .  $Y \in [0, 1]$  is a gas expansion factor for the gas flow and  $P_s$  is the separator pressure, i.e. the pressure downstream the choke.

### 2.3 Numerical Implementation

The drift flux model described above was implemented using a fully implicit Backwards Time-Central Space (BTCS) finite differences numerical scheme with an explicitly derived Jacobian as described in Aarsnes et al. (2014b).

Define the state vector, to be made up of the conservative variables  $m, n$  and  $I = mv_L + nv_L$ ,  $X = [m \ n \ I]^T$ . For each of the states we use the following definition for finite differences,

$$m_i^k = m(k\Delta t, i\Delta x), \quad \text{etc.}$$

where  $i = 0, 1, \dots, N$  and  $k = 0, 1, \dots$ . We arrange the terms into a vector

$$X_k = [m_1^k, m_2^k, \dots, m_N^k, n_1^k, \dots, n_N^k, I_1^k, \dots, I_N^k].$$

Consequently, propagating the states in time from  $X_k$  to  $X_{k+1}$  equates to solving a set of nonlinear equations that are implicit in  $X_{k+1}$ , which we denote as

$$F(X_{k+1}, X_k) = 0, \quad F: \mathbb{R}^{3N} \times \mathbb{R}^{3N} \rightarrow \mathbb{R}^{3N}. \quad (19)$$

These are solved using Newton steps which require the inverse of the Jacobian of  $F$  w.r.t.  $X_{k+1}$  denoted  $F_{X_{k+1}}$ .

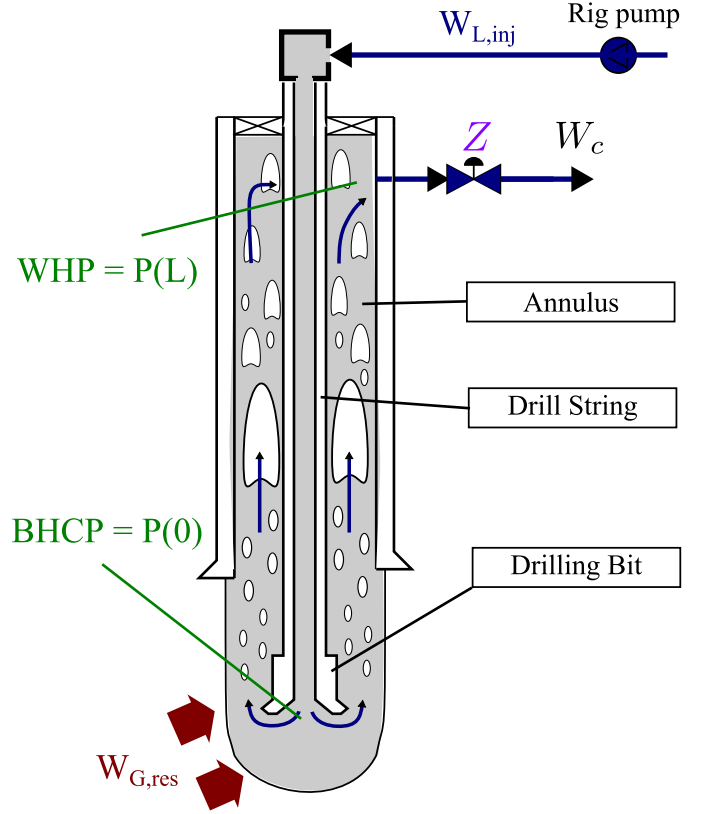


Fig. 1. Drilling process schematic for UBD.

We note that the existence of this inverse is guaranteed by the  $1/\Delta t$  terms making up the diagonal of  $F_{X_{k+1}}$ .

### 3. UNSCENTED KALMAN FILTER

The implemented drift-flux model based on equations (5)-(18), although solved implicitly, can conceptually be represented as

$$X_k = f(X_{k-1}, \theta) + q_k \quad (20)$$

$$y_k = h(X_k) + r_k \quad (21)$$

where  $q_k \sim N(0, Q_{k-1})$  is the zero mean Gaussian process noise and model error, and  $r_k \sim N(0, R_k)$  is the zero mean Gaussian measurement noise.

The Kalman filter based on a linearized model was developed to estimate both state and parameter of the system usually known as an augmented Kalman filter. The UKF technique has been developed to work with nonlinear system without using an explicit linearization of the model (Julier et al. (2000); Julier and Uhlmann (2004); van der Merwe (2004)). The UKF estimates the mean and covariance matrix of the estimation error with a minimal set of sample points (called sigma points) around the mean by using a deterministic sampling approach known as the unscented transform. The nonlinear model is applied to sigma points to predict uncertainty instead of using a linearization of the model. More details can be found in (Julier and Uhlmann (2004); van der Merwe (2004); Simon (2006)).

Dual and joint UKF techniques are two common approaches for estimation of parameters and state variables simultaneously. The dual UKF method uses another UKF for parameter estimation so that two filters run sequentially in every time step; the state estimator updates with

new measurements, and then the current estimate of the state is used in the parameter estimator. The joint UKF augments the original state variables with parameters and a single UKF is used to estimate augmented state vector. In this paper, the joint UKF is used. The augmented state vector is defined by  $x^a = [X, \theta]$ . The state-space equations for the augmented state vector at time instant  $k$  are written as:

$$\begin{bmatrix} X_k \\ \theta_k \end{bmatrix} = \begin{bmatrix} f(X_{k-1}, \theta_{k-1}) + q_k \\ \theta_{k-1} \end{bmatrix} = f^a(X_{k-1}, \theta_{k-1}) + q_k^a \quad (22)$$

In the following simulations, it is assumed that only bottom-hole pressure ( $P(0)$ ) and liquid and gas rate at the outlet are measured. The joint UKF estimates the states, production constant gas and slip parameters ( $S, K$ ) simultaneously.

#### 4. EXTENDED KALMAN FILTER

For the implementation of an Extended Kalman Filter, to be used for comparison we need the Jacobian of the explicit formulation of the system equation. A first order Taylor series expansion around the trajectory  $\bar{X}$ , noting that  $F(\bar{X}_{k+1}, \bar{X}_k) = 0$ , yields

$$F_{X_{k+1}}(\bar{X}_{k+1}, \bar{X}_k)\tilde{X}_{k+1} + F_{X_k}(\bar{X}_{k+1}, \bar{X}_k)\tilde{X}_k = 0. \quad (23)$$

where  $F_{X_k}(\bar{X}_{k+1}, \bar{X}_k)$  is  $F$  with respect to a  $X_k$ . Hence, for the system Jacobian, we get

$$J = -F_{X_{k+1}}^{-1}(\bar{X}_{k+1}, \bar{X}_k)F_{X_k}(\bar{X}_{k+1}, \bar{X}_k)$$

where the partial derivatives are evaluated at the trajectory. We recognize  $F_{X_{k+1}}$  to be the Jacobian, previously discussed, the inverse of which is known to exist.

#### 5. SIMULATION RESULTS

##### 5.1 Simulation with perfect model data

First, the presented DFM, (5)-(15) was used to create the measurements and true states in this simulation study. In this case the estimated states and parameters, in several configurations of unknown parameters to be estimated, converged to the true states (results not shown). Convergence transients were typically 0.5 hours for the UKF and 1.5 hours for the EKF. Of significantly more interest, however, is how the estimators performs in a more realistic setting where we would have model errors to deal with. Such a scenario is considered next.

##### 5.2 Simulation with OLGA data

The parameter values for the simulated well and reservoir are summarized in Table 1. These parameters are used from the OLGA simulator. The OLGA dynamic multiphase flow simulator is a high fidelity simulation tool which has become the de facto industry standard in oil and gas production, see Bendiksen et al. (1991). The measurements have been synthetically generated by using the OLGA dynamic multiphase flow simulator.

In the following, a measurement sampling interval of 10 seconds were used, and the model was run with time steps of 10 seconds using different spatial discretization steps ( $N = 6, 12, 20$ ). The initial values for the estimated

Table 1. PARAMETER VALUES FOR WELL AND RESERVOIR

Name	DFM	Unit
Reservoir pressure ( $p_{res}$ )	279	bar
Collapse pressure ( $p_{coll}$ )	155	bar
Well total length ( $L_{tot}$ )	2530	m
Drill string outer diameter ( $D_d$ )	0.1206	m
Annulus inner diameter ( $D_a$ )	0.1524	m
Liquid flow rate ( $w_{l,d}$ )	13.33	kg/s
Gas flow rate ( $w_{g,d}$ )	0	kg/s
Liquid density ( $\rho_L$ )	1000	kg/m <sup>3</sup>
Production constant of liquid ( $K_L$ )	0	kg/Pa
Gas average temperature ( $T$ )	285.15	K
Average angle ( $\Delta\theta$ )	$\pi/2$	rad
Choke constant ( $K_c$ )	0.0053	m <sup>2</sup>

Table 2. Choke opening used in this scenario

Time	Choke Opening
0-1 h	10 %
1-2 h	8 %
2-6 h	7 %
6-8 h	6 %
8-10 h	5.5 %

production constant of gas is ( $\hat{K}_G = 0.08$  kg/s/bar). UKF parameters are determined empirically ( $\kappa = 0$ ,  $\beta = 2$ ,  $\alpha = 0.00001$ ). The measurement noise covariance matrix is  $R = \text{diag}[0.01, 0.0004, 0.04]$ . The parameter covariance matrix uses in this simulation for both EKF and UKF is

$$Q_p = \text{diag}[10^{-4}, 2 * 10^{-6}, 2 * 10^{-5}]$$

$$p = [K_G, K, S]$$

This paper uses the same simulation scenario as Aarsnes et al. (2014a), considering UBD operation of a vertical well drilled into a dry gas reservoir (i.e.  $W_{L,res} = K_L = 0$ ). The scenario in this simulation is as follows. First drilling in a steady-state condition is initiated with the choke opening of 10 % , then the choke is closed to 8 % at 1 hour. After 2 hours, the choke is closed to 7 %. After 3.5 hours, there is a linear and sharp increase in the production constant of gas from 0.072 kg/s/bar to 0.12 kg/s/bar (change of reservoir height). Then the choke is closed to 6 % at 6 hours, and after 8 hours, the choke is closed to 5.5 %. The choke opening of this simulation scenario is summarized in Table 2.

The estimation of the production constant of gas from the reservoir into the well for different spatial discretization steps for both UKF and EKF is shown in Figure 2. The estimation algorithms are quite fast to detect and track changing at production constant of gas. However, there is a small deviation between the estimated and actual value of the production constant of gas. The number of steps in the spatial discretization does not have a significant effect on the accuracy of estimation, although the results show that decreasing number of steps can improve the convergence rate.

Figures 3 and 4 show the estimated slip parameters  $K$  and  $S$  for different spatial discretization steps for both UKF and EKF, respectively.

Figure 5 shows the estimation of the production constant of gas with different fixed slip parameters by using UKF with 6 spatial discretization steps. The results show that estimation of the slip parameters can improve accuracy of the estimation of the production constant of gas. The measured bottom-hole pressure and choke pressure

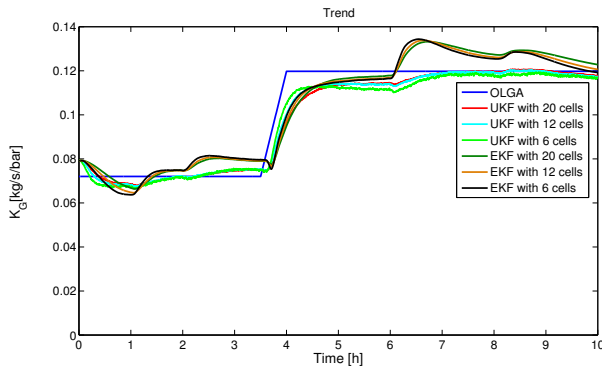


Fig. 2. Estimating production constant of gas with different spatial discretization steps

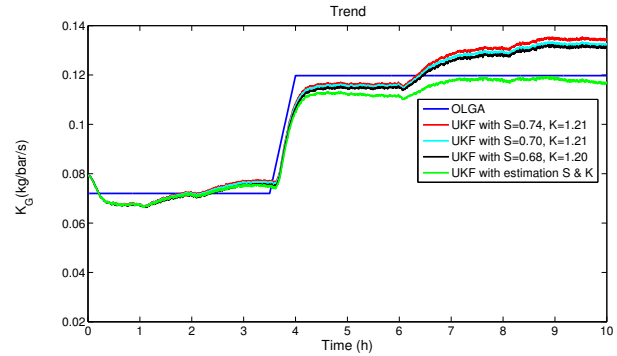


Fig. 5. Estimating production constant of gas with fixed slip parameters

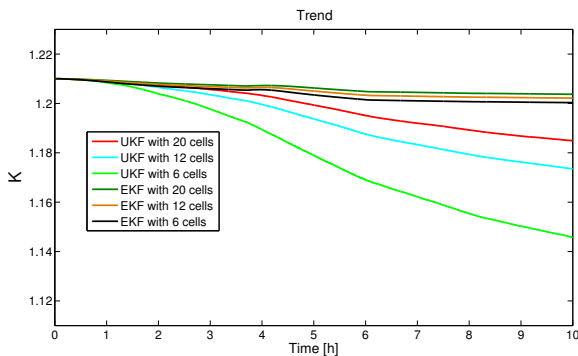


Fig. 3. Estimating slip parameter (K) for different spatial discretization steps

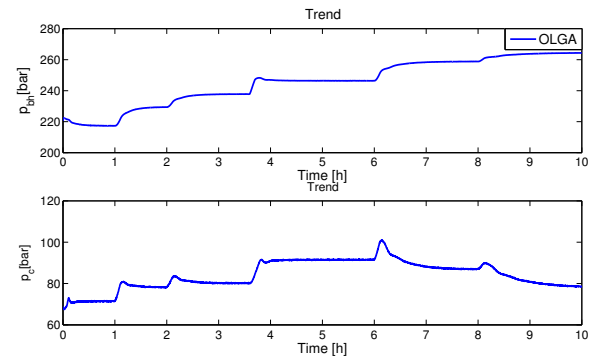


Fig. 6. Bottom-hole pressure and choke pressure

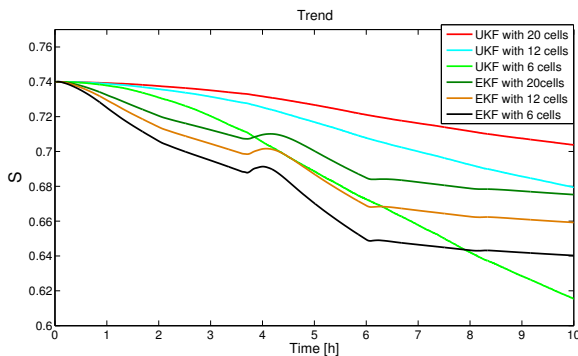


Fig. 4. Estimating slip parameter (S) for different spatial discretization steps

is illustrated in Figure 6.

The runtime of the simulations for different spatial discretization steps for both UKF and EKF are summarized in Table 3 by using 3.00 GHz Processor with 4 GB RAM running MATLAB, the runtime of the simulations for EKF are less than runtime of the simulations for UKF, but we emphasize that the implementation is not optimized for computational efficiency.

In this paper, performance of these adaptive observers is evaluated through the root mean square error (RMSE) metric for the parameter  $K_G$ . The RMSE metric for UKF and EKF for different spatial discretization steps are summarized in Table 4. According to the RMSE metric table, UKF with fewer cells in the spatial discretization has a better performance than UKF with larger spatial discretiza-

Table 3. Simulation runtime for different spatial discretization steps

Number of Cells	UKF (seconds)	EKF(seconds)
6	630.38	63.88
12	1110.82	67.27
20	2326.35	78.16

Table 4. RMSE metric for estimate of  $K_G$

Number of Cells	UKF	EKF
6	$4.8 \times 10^{-3}$	$8.2 \times 10^{-3}$
12	$4.8 \times 10^{-3}$	$8 \times 10^{-3}$
20	$5.16 \times 10^{-3}$	$8.3 \times 10^{-3}$

tion steps and EKF with different spatial discretization steps for PI estimation, although the number of steps in the spatial discretization does not have a significant effect on the accuracy of estimation.

## 6. CONCLUSION

In this paper, the joint UKF and EKF have been applied to the simplified drift-flux model for different spatial discretization steps to estimate the distributed unmeasured states, geological properties of the reservoir (PI) and slip parameters ( $S, K$ ) during UBD operations. Simulation results demonstrated reasonable performance of the joint UKF and EKF to detect and track a changing gas production coefficient using a simulated scenario with OLGA. Even though the simulation scenario is somewhat idealized the results are encouraging. The number of spatial discretization steps was found to not have a significant

effect on accuracy of estimation. The UKF was also found to yield faster and more accurate estimates than the EKF.

#### ACKNOWLEDGEMENTS

The authors gratefully acknowledge the financial support provided to this project through the Norwegian Research Council and Statoil ASA (NFR project 210432/E30 Intelligent Drilling).

#### REFERENCES

- Aarsnes, U.J.F., Aamo, O.M., Di Meglio, F., and Kaasa, G.O. (2014a). Fit-for-purpose modeling for automation of underbalanced drilling operations. In *SPE/IADC Managed Pressure Drilling & Underbalanced Operations Conference & Exhibition*.
- Aarsnes, U.J.F., Di Meglio, F., Evje, S., and Aamo, O.M. (2014b). Control-oriented drift-flux modeling of single and two-phase flow for drilling. In *Proc. ASME 2014 Dyn. Syst. Control Conf.*
- Bendiksen, K.H., Maines, D., Moe, R., and Nuland, S. (1991). The dynamic two-fluid model olga: Theory and application. *SPE production engineering*, 6(02), 171–180.
- Bloemen, H., Belfroid, S., Sturm, W., and Verhelst, F. (2006). Soft sensing for gas-lift wells. *SPE J.*, 11(December), 454–463. doi:10.2118/90370-PA.
- Di Meglio, F., Bresch-Pietri, D., and Aarsnes, U.J.F. (2014). An adaptive observer for hyperbolic systems with application to underbalanced drilling. In *IFAC World Congress 2014*, 11391–11397.
- Evje, S. (2011). Weak solutions for a gas-liquid model relevant for describing gas-kick in oil wells. *SIAM J. Math. Anal.*, 43(4), 1887–1922. doi:10.1137/100813932.
- Evje, S. and Fjelde, K.K. (2002). Hybrid flux-splitting schemes for a two-phase flow model. *Journal of Computational Physics*, 175, 674–701.
- Graham, R.A. and Culen, M.S. (2004). Methodology For Manipulation Of Wellhead Pressure Control For The Purpose Of Recovering Gas To Process In Underbalanced Drilling Applications. In *Proc. SPE/IADC Underbalanced Technol. Conf. Exhib.* Society of Petroleum Engineers, Houston, Texas. doi:10.2118/91220-MS.
- Gryzlov, A.N. (2011). *Model-based estimation of multiphase flows in horizontal wells*. Ph.D. thesis, Technische Universiteit Delft.
- Julier, S.J. and Uhlmann, J.K. (2004). Unscented filtering and nonlinear estimation. *Proceedings of the IEEE*, 92(3), 401 – 422.
- Julier, S.J., Uhlmann, J.K., and Durrant-Whyte, H.F. (2000). A new method for the nonlinear transformation of means and covariances in filters and estimators. *IEEE Transactions on Automatic Control*, 45(3), 477–482.
- Lage, A., Nakagawa, E., Time, R., Vefring, E., and Rommetveit, R. (1999). Full-scale experimental study for improved understanding of transient phenomena in underbalanced drilling operations. In *SPE/IADC Drilling Conference*, 52829-MS. Society of Petroleum Engineers, Amsterdam, Netherlands.
- Lorentzen, R., Nævdal, G., and Lage, A. (2003). Tuning of parameters in a two-phase flow model using an ensemble kalman filter. *International Journal of Multiphase Flow*, 29(8), 1283–1309.
- Lorentzen, R.J., Stordal, A., Nævdal, G., Karlsen, H.A., and Skaug, H.J. (2014). Estimation of Production Rates With Transient Well-Flow Modeling and the Auxiliary Particle Filter. *SPE J.*, 19(01), 172–180. doi:10.2118/165582-PA.
- Luo, X., Lorentzen, R.J., Stordal, A.S., and Nævdal, G. (2014). Toward an enhanced bayesian estimation framework for multiphase flow soft-sensing. *Inverse Problems*, 30(11), 114012.
- Nikoofard, A., Johansen, T.A., and Kaasa, G.O. (2014a). Design and comparison of adaptive estimators for underbalanced drilling. In *American Control Conference (ACC)*, 5681–5687. IEEE, Portland, Oregon, USA.
- Nikoofard, A., Johansen, T.A., and Kaasa, G.O. (2014b). Nonlinear moving horizon observer for estimation of states and parameters in under-balanced drilling operations. In *ASME 2014 Dynamic Systems and Control Conference*. American Society of Mechanical Engineers.
- Nygaard, G., Nævdal, G., and Mylvaganam, S. (2006). Evaluating nonlinear kalman filters for parameter estimation in reservoirs during petroleum well drilling. In *IEEE International Conference on Control Applications*, 1777–1782. IEEE.
- Nygaard, G. and Nævdal, G. (2006). Nonlinear model predictive control scheme for stabilizing annulus pressure during oil well drilling. *Journal of Process Control*, 16(7), 719–732.
- Nygaard, G.H., Imsland, L.S., and Johannessen, E.A. (2007). Using nmpc based on a low-order model for controlling pressure during oil well drilling. In *8th International IFAC Symposium on Dynamics and Control of Process Systems*, volume 1, 159–164. Mexico.
- Shi, H., Holmes, J., Durlofsky, L., Aziz, K., Diaz, L., Alkaya, B., and Oddie, G. (2005). Drift-Flux Modeling of Two-Phase Flow in Wellbores. *SPE J.*, 10(1), 24–33. doi:10.2118/84228-PA.
- Simon, D. (2006). *Optimal state estimation: Kalman, H infinity, and nonlinear approaches*. Wiley. com.
- Storkaas, E., Skogestad, S., and Godhavn, J.M. (2003). A low-dimensional dynamic model of severe slugging for control design and analysis. In *11th International Conference on Multiphase flow (Multiphase03)*, 117–133.
- Teixeira, B.O., Castro, W.S., Teixeira, A.F., and Aguirre, L.a. (2014). Data-driven soft sensor of downhole pressure for a gas-lift oil well. *Control Eng. Pract.*, 22, 34–43. doi:10.1016/j.conengprac.2013.09.005.
- van der Merwe, R. (2004). *Sigma-Point Kalman Filters for Probabilistic Inference in Dynamic State-Space Models*. Ph.D. thesis, Oregon Health & Science University.
- Vefring, E.H., Nygaard, G., Lorentzen, R.J., Nævdal, G., Fjelde, K.K., et al. (2003). Reservoir characterization during ubd: Methodology and active tests. In *IADC/SPE Underbalanced Technology Conference and Exhibition*. Society of Petroleum Engineers.
- Vefring, E.H., Nygaard, G.H., Lorentzen, R.J., Nævdal, G., Fjelde, K.K., et al. (2006). Reservoir characterization during underbalanced drilling (ubd): methodology and active tests. *SPE Journal*, 11(02), 181–192.
- Wan, E.A. and van der Merwe, R. (2002). *The Unscented Kalman Filter, in Kalman Filtering and Neural Networks* (ed S. Haykin), chapter 7. John Wiley & Sons, New York, USA.